American Journal of Applied Scientific Research
2019; 5(3): 56-61
http://www.sciencepublishinggroup.com/j/ajasr
doi: 10.11648/j.ajasr.20190503.12
ISSN: 2471-9722 (Print); ISSN: 2471-9730 (Online)

Review Article

A Theoretical Approach: Effects of *Mn* Substitution in *Cobalt* Ferrite

Md. Ziaul Ahsan[1], Md. Aminul Islam[2]

[1]Military Institute of Science and Technology, Mirpur Cantonment, Dhaka, Bangladesh

[2]Department of Physics, Bangladesh University of Engineering and Technology, Dhaka, Bangladesh

Email address:
ahsanziaul@sh.mist.ac.bd (Md. Z. Ahsan), maislam.buet.phy@gmail.com (Md. A. Islam)

To cite this article:
Md. Ziaul Ahsan, Md. Aminul Islam. A Theoretical Approach: Effects of *Mn* Substitution in *Cobalt* Ferrite. *American Journal of Applied Scientific Research.* Vol. 5, No. 3, 2019, pp. 56-61. doi: 10.11648/j.ajasr.20190503.12

Received: July 25, 2019; **Accepted**: August 13, 2019; **Published**: November 4, 2019

Abstract: This paper reports on the effect of Mn substitution in cobalt ferrite to explore the probable correlation among the structural, magnetic, and magneto-mechanical properties by a theoretical approach. Three compositions of *Mn* doped Cobalt ferrites at different Mn concentration (x) = 0.125, 0.25, 0.375, 0.5 have been undertaken for their analytical study to understand the correlation among the aforesaid properties. In this approach, an empirical equation has been formulated based on idealistic cation distribution in tetrahedral and octahedral sites of cobalt ferrite at room temperature. The hopping lengths and bond lengths have also been estimated using the corresponding Stanley's equations in idealistic condition. The estimated lattice constant is found to decrease and effective magnetic moment μ_{ferri} to increase with the *Mn* content, substituted for *Co* in the octahedral site due to increased A-B interactions. This increasing effect of Mn content in cobalt ferrite may be significant to the tunability of the Curie temperature, T_C and may have an influence on superparamagnetism (SPM). On the other hand, the compositions where *Mn* substituted for *Fe* may increase the porosity due to their increased bond lengths with Mn content and thus may optimize them for applications in the environmental (gas) sensors. However, the analysis of the predicted effects of Mn and correlation thereon is completely based on the theoretical approach and thereby need experimental verification to confirm and supplement them.

Keywords: Lattice Constant, Hopping Length, Bond Length, Effective Magnetic Moment, Porosity

1. Introduction

Cobalt ferrites are reported as the best-known examples of the hard ferrite materials because of their excellent chemical stability, mechanical hardness, reasonable saturation magnetization and high magnetocrystalline anisotropy [1]. An extremely wide variety of total solid solution enables this cobalt ferrite to be strongly modified keeping the ferrite structure almost unchanged, which leads to a series of investigations on Mn doped cobalt ferrites. By the time, intensive researches towards the discovery and development of cobalt ferrite nanoparticles with doped and composite kind have been made them possible to be used in diversified fields of application such as electronic devices, ferrofluids, drug delivery system, magnetic resonance imaging, microwave devices and high-density information storage. These applications are mostly based on magnetic and electrical behaviors and their alteration or tuning, depending on the ionic radii of doped atoms in the host lattice and their particle size. Recently, tuning of fundamental magnetic properties of doped cobalt ferrite by adjusting dopant content, sintering temperature and their size have received renewed attention across the world to optimize them both in sensor and high frequency applications. A substantial and almost linear decrease of the Curie temperature T_C but the modest decline of magnetization is observed with *Mn* content, substituted for *Fe* [2-6]. The dependence of structural and magnetic properties on dopant content, sintering temperature has been studied [7]. But the tunability to adjust dopant content to an optimum value of magnetic properties at which the operating temperature and external magnetic field can cause to flip the magnetic transition from one state to another is not conspicuous, which demands a theoretical study to predict at room temperature. Lattice constants of $Co_{1-x}Mn_xFe_2O_4$,

$CoMn_xFe_{2-x}O_4$ and $Co_{1+x}Mn_xFe_{2-x}O_4$have been estimated by an empirical equation with different *Mn* content (*x = 0.125, 0.250, 0.375, 0.500*) at room temperature. Using Stanley's equations, other structural parameters such as bond lengths, hopping lengths, and density have also been estimated from the respective lattice constants. The obtained values of those parameters are used for analytical studies of structural and magnetic properties, and effects thereon. Keeping the above in view, the objective of this paper is to have comprehensive theoretical studies on the effects of *Mn* substitution in *Cobalt* ferrites for understanding their tenable behavior and tuning of fundamental magnetic properties by adjusting *Mn* content for optimizing them in advanced applications.

2. Theoretical

2.1. Structural Properties

2.1.1. Structure

Bulk $CoFe_2O_4$possesses an inverse spinel structure in which ideally half of the trivalent ferric cations (Fe^{3+}) are positioned on A site and the other half Fe^{3+}cations and all divalent cobalt cations (Co^{2+}) on B site as depicted in Figure 1. An inverse spinel unit cell is made up of eight face-centered cubic (*fcc*) cells of oxygen ions in the configuration 2×2×2. So it is a big structure consisting of 32 oxygen ions, 8 *A* cations and 16 *B* cations. Accordingly, $CoFe_2O_4$ has also 8 sublattices (molecules) in its unit cell with 32 anions and 24 cations, which are ideally distributed at room temperature as shown in Table 1.

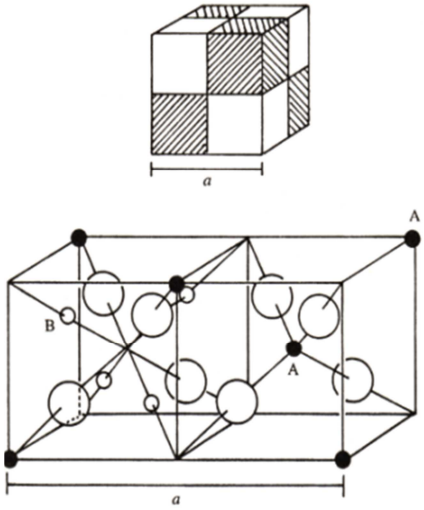

Figure 1. *The unit cell of the inverse (B) [AB]O_4 Spinel contains 8 sublattices.(Molecules adopted from Wiki book).*

Table 1. *Anion and cation distribution in the ideal inverse spinel structure.*

Constituents	Tetrahedral*(A-O)* SL	Octahedral *(B-O)* SL	Number of sublattice in each unit cell
Fe^{3+}	8	8	8
Co^{2+}	-	8	
O^{2-} *(R-O)*	8		Remaining anions in the unit cell

2.1.2. Structural Parameters

In order to understand the correlation of lattice constant, bond lengths, hopping lengths of *A* and *B* sites and density with *Mn* content of the compositions $Co_{1-x}Mn_xFe_2O_4$, $CoMn_xFe_{2-x}O_4$ and $Co_{1+x}Mn_xFe_{2-x}O_4$, where *x = 0.125, 0.250, 0.375, 0.500*, the following empirical equation of lattice constant *a,* is formulated depending upon the distribution of cations and anions in inverse spinel structure as mentioned in table 1 at room temperature:

$$a = \sqrt[3]{\langle\{(V_{A-O}) + [V_{B-O}] + V_{R-O}\} \times 8\ sublatticesinaspinelunitcell\rangle} - u \quad (1)$$

Where,

$$V_{A-O} = No.A - cation \times \frac{4}{3}\pi r_A^3 = \text{Volume of tetrahedral sublattice}$$

$$V_{B-O} = No.B - cation \times \frac{4}{3}\pi r_B^3 = \text{Volume of octahedral sublattice}$$

$$V_{R-O} = No.R - anion \times \frac{4}{3}\pi r_O^3 = \text{Volume of remaining oxygen ions}$$

u = Oxygen ion positional parameter, arising from displacement of oxygen along the direction perpendicular to the diagonal of the cube, and for the ideal structure, it is equal to 3/8 (=0.375). And r_A, r_B, and r_o are the ionic radius of A cation, B cation, and oxygen ion respectively, the values of constituent cations and oxygen anion obtained from the literature.

Using this equation-1, lattice constant '*a'* for *x =0.125, 025, 0.375* and *0.500* of each composition has been estimated. The value of *a*, for *x = 0* found to be ~8.3702 Å, which is comparable to~8.3802Å as obtained from *XRD* pattern [8, 14] but ~8.0966 Åas estimated from *Vegard's* formula of the same compound. All other structural parameters like tetrahedral and octahedral bond lengths and hopping lengths have been estimated by respective Stanley's equation (equations 2, 3 and 4) for each composition. The corresponding Stanley's equations are given below:

$$A - O = \left(u - \frac{1}{4}\right) a\sqrt{3}\text{Å} \quad \text{For tetrahedral bond length} \quad (2)$$

$$B-O=\left(\frac{5}{8}-u\right)a\ \text{Å}\quad\text{For octahedral bond length}\qquad(3)$$

$$(L)=\frac{a\sqrt{3}}{4}\text{Å}\quad\text{For tetrahedral hopping length}\qquad(4)$$

$$[L]=\frac{a\sqrt{2}}{4}\text{Å}\quad\text{For octahedral hopping length}$$

2.1.3. Density and Porosity

Using formula$\frac{8M}{Aa^3}$, density has also been estimated for bulk $CoFe_2O_4$ ferrite with a mass of 234.63 g mol^{-1}. The estimated density (usually known as X-ray density) is 5.315 gcm^{-3} and found to be almost in agreement with the literature value [4, 8]. The porosity is defined as$P=(1-\rho_b/\rho_x)$, where, the bulk density ρ_b depends on the dimension of the sample pellet, which can be estimated by the formula:$\rho_b=m/\pi r^2h$, here, *m* is the mass (kg), *r* is the radius (m) and *h* is the height of the sample. For a typical disk-shaped sample of 20mg each (7.6 mm diameter and 1 mm thickness), the estimated bulk density found to be~4.41g cm^{-3}, which leads to having the porosity of this sample~17.03%. However, the values of these structural parameters as estimated above may vary owing to redistribution of cations among the *A* and *B* sites depending on dopant (*Mn*) content, synthesizing technique, calcination and sintering temperature, and also on size and shape of particles when they reduce to the nanoscale.

2.2. Magnetic Properties

2.2.1. Magnetic Moment

Below T_C, ferric ions, Fe^{3+} in *A* site have aligned magnetic moment (parallel spins) resulting ferromagnetism and produces net magnetic moment, while the cobalt ions Co^{2+} and ferric ions Fe^{3+} in *B* site have anti-parallel alignment that results in antiferromagnetism and balances or cancels out net magnetic moment depending upon the number of unpaired spins as reported in case of magnetite [9]. Accordingly, the situation may be hypothetically depicted in Figure 2.

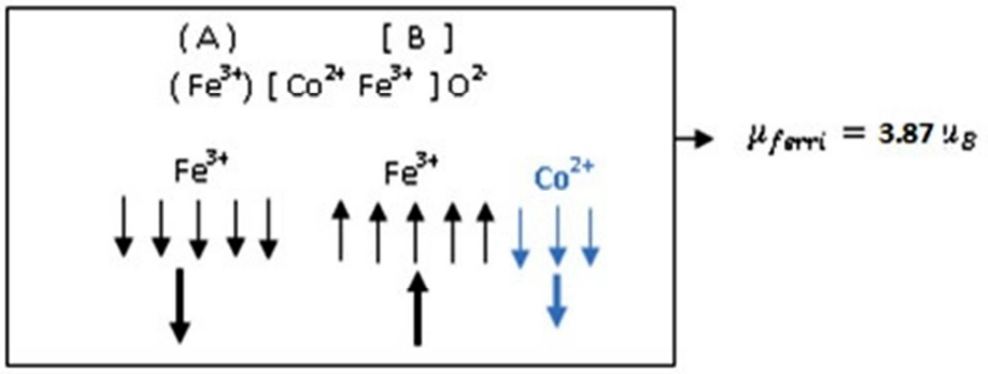

Figure 2. *Hypothetical schematic view of the ferromagnetic and antiferromagnetic alignment of spins in A and B sites.*

Hence, the exchange interaction between *A* and *B* sites lead $CoFe_2O_4$ ferrite to possess ferrimagnetic behavior due to magnetic moments of bivalent cations $M^{2+}(Co^{2+})$ in the *B* position as reported in the literature [9]. Accordingly, the effective magnetic moment μ_{ferri} for inverse spinel structure may be estimated by the following equation, modified from the formula of normal spinel structure [10] as:

$$\mu_{ferri}=\mu_B-\mu_A=[\mu_{M^{2+}}+\mu_{Fe^{3+}}]^B-[\mu_{Fe^{3+}}]^A\ \text{ for }\ CoFe_2O_4\qquad(5)$$

Where, μ_A and μ_B magnetic moments of *A* and *B* sites respectively, and $\mu_{M^{2+}}(3.87\mu_B)$ and $\mu_{Fe^{3+}}(5.91\mu_B)$ magnetic moments of $M^{2+}(Co^{2+})$ and Fe^{3+}ions respectively. The values within braces have been estimated from the relation of spin only magnetic moment ($\mu=\{n(n+2)\}^{1/2}\mu_B$). So, the effective magnetic moment μ_{ferri} found to be$3.87\mu_B$ for bulk $CoFe_2O_4$ ferrite as estimated by the above equation. When the dopants (Mn^{2+}) are incorporated in the Cobalt ferrites, then the formula for effective magnetic moment μ_{ferri} might take the following forms:

$$\mu_{ferri}=[(1-x)\mu_{Co^{2+}}+x\mu_{Mn^{2+}}+\mu_{Fe^{3+}}]^B-[\mu_{Fe^{3+}}]^A\ \text{for}\ Co_{1-x}Mn_xFe_2O_4\qquad(6)$$

$$\mu_{ferri}=[\mu_{Co^{2+}}+x\mu_{Mn^{2+}}+(1-x)\mu_{Fe^{3+}}-\mu_{Fe^{3+}}]^B-[(1-x)\mu_{Fe^{3+}}]^A\ \text{for}\ CoMn_xFe_{2-x}O_4\qquad(7)$$

$$\mu_{ferri}=[(1+x)\mu_{Co^{2+}}+x\mu_{Mn^{2+}}+(1-x)\mu_{Fe^{3+}}-\mu_{Fe^{3+}}]^B-[(1-x)\mu_{Fe^{3+}}]^A\ \text{for}\ Co_{1+x}Mn_xFe_{2-x}O_4\qquad(8)$$

Where, *x* represents the substitution level of *Mn* content in the parent sample of cobalt ferrite and $\mu_{Mn^{2+}}(4.898\mu_B)$ the spin alone magnetic moment of Mn^{2+}. Notable that, the measured value may be different depending upon the ionic redistribution during synthesizing and sintering temperature as reported in various literature.

2.2.2. Size Effect on Magnetization and SuperPara Magnetism (SPM)

Usually, bulk $CoFe_2O_4$ ferrite is of multi-domains like magnetite, Fe_2O_4. But when the particle size of cobalt ferrites reduces to 20 nm or below, their multi-domains turn into a single domain particle. As a result, the surface-volume ratio

found to increase, which in turn increases the internal pressure and reduces the external pressure on the particles. According to Laplace, this difference in pressure variables (internal and external) is inversely proportional to the radius of the particle and directly proportional to the surface tension (as mathematically expressed by an equation $P_{internal} - P_{external} = P_{laplace} = \frac{2\gamma}{r}$) owing to surface chemistry. Because of reduced external pressure, the particles get swell and thus causes the volume expansion, which ultimate to increase the lattice constant without changing the crystal structure of the unit cell as reported for Fe_2O_4. This change of a found to be insignificant in their structural properties but may have significance in the tuning of magnetic properties. With the decrease of particle size, the amount of exchange coupled spins, which resists the spontaneous magnetic reorientation, may decrease and tending towards paramagnetic or superparamagnetic magnetization as reported for Fe_2O_4 [11]. This exchange coupling of spins expected to depend on the hopping lengths (L) and [L], which indicates the correlation between saturation magnetization and lattice constant' *a'*. So, the paramagnetic behavior in bulk $CoFe_2O_4$ferrites and superparamagnetic behavior in their nanoparticles may be made tunable with the lattice parameter and in turn dopant (*Mn*) content. Superparamagnetic behavior is the exclusive property of magnetic nanoparticles and found to arise when the thermal energy fluctuations or an applied field can easily move magnetic moments away from the easy axis (The preferred crystallographic axes for the magnetic moment are to point along). Then each particle behaves like paramagnetic atom but with giant magnetic moment owing to sustained magnetic order [10]. The giant magnetic moment may be thought of as the determining factor of superparamagnetism in $CoFe_2O_4$ ferries, which may depend on the hopping lengths and in turn, on lattice constant *'a'*.

3. Result and Discussion

3.1. Structural Properties

The estimated values of lattice constant a, tetrahedral hopping length (L), octahedral hopping length [L], tetrahedral bond length, A-O and octahedral bond length B-O found to increase for $CoMn_xFe_{2-x}O_4$ and $Co_{1+x}Mn_xFe_{2-x}O_4$ but to decrease for $Co_{1-x}Mn_xFe_{2-x}O_4$ with Mn content as depicted in graphs of Figures 3, 4 and 5 respectively. This increase or decrease of a can be attributed to the ionic radius of Mn^{2+}(0.66A°) compared to substituted ions Co^{2+}(0.71A°) or Fe^{3+}(0.49A°) depending on composition as reported for the case of Zn^{2+} substitution for Co^{3+} [12]. It implies that there is a correlation between lattice constant and ionic radius [13], which may be expressed by the empirical equation as: $a(x) = a_0 \pm mx$, where$a\ (x)$ is the lattice constant for any value ofx (Mn content), a_0 the lattice constant at x =0 (for parent sample) and m is the slope to determine the rate of change of a with x. Notable here, a similar equation may be applied for hopping lengths and bond lengths as well. However, the relation as established here between the lattice constant and the concentration of dopant (Mn) is completely based on a theoretical approach. This relation may not be the same in the experimental approach due to the ionic redistribution between A and B sites depending on synthesizing technique, calcination temperature, and particle size as mentioned above. So, a series of investigations is required under different conditions.

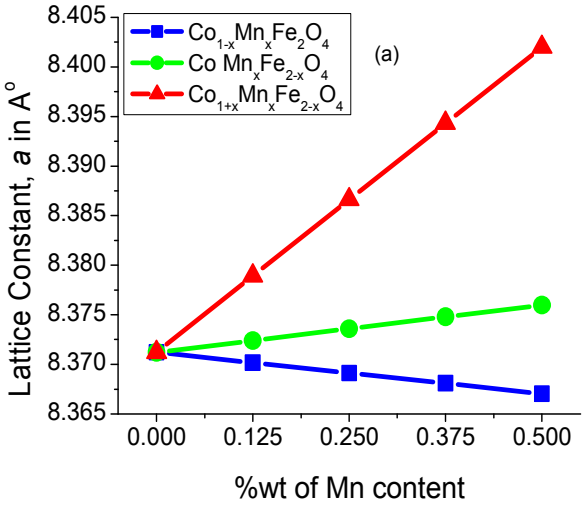

Figure 3. *Lattice constant, a as a function of Mn content.*

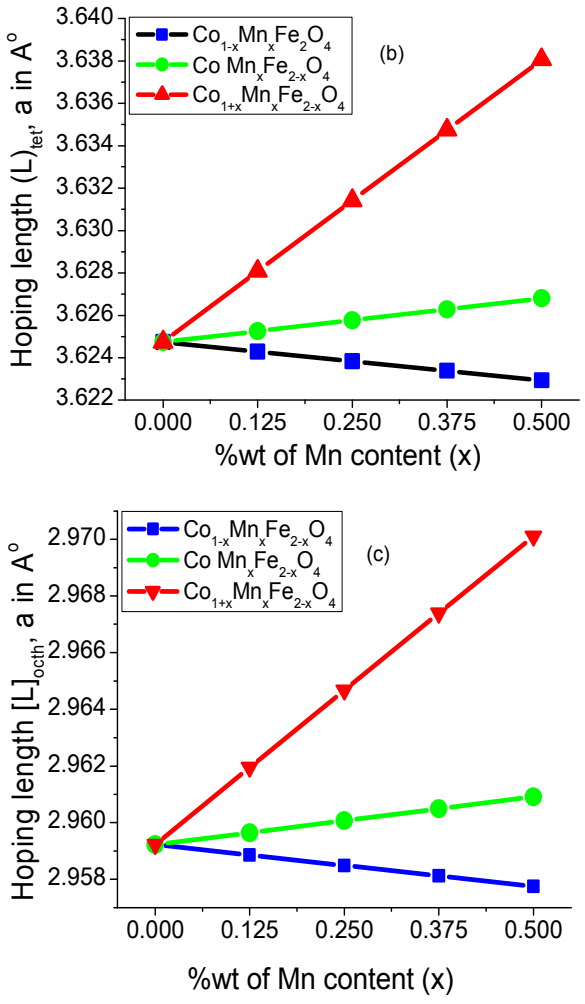

Figure 4. *Graph as a function of Mn content for hopping lengths (L) and [L].*

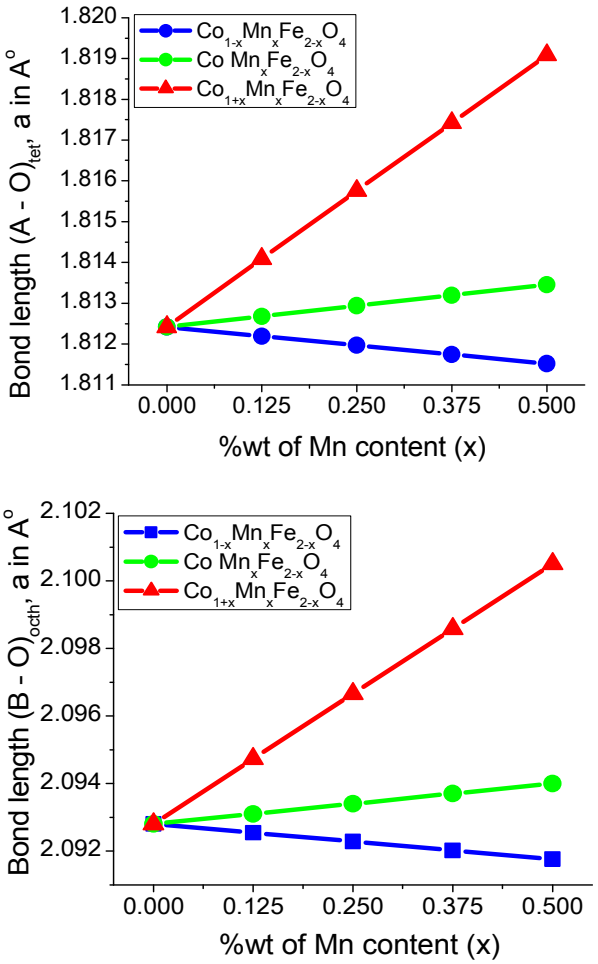

Figure 5. *Graph as a function of Mn content for bond lengths A-O and B-O.*

3.2. Magnetic Properties

Figure6 shows the variation of the estimated effective magnetic moment, μ_{ferri} as a function of Mn content (x). The increase of *a*, on the other hand, increases (L) and [L], which may reduce the super-exchange interactions between magnetic ions of *A* and *B* sites at room temperature and resulting this decrease in the effective magnetic moment μ_{ferri} for $CoMn_xFe_{2-x}O_4$ with *Mn* content(x) and thereby leading to decrease of saturation magnetization, M_s as reported [12]. Conversely, the decrease of *a* causes shortening in (L) and [L] for $Co_{1-x}Mn_xFe_2O_4$, which may enhance the super-exchange interactions between magnetic ions of *A* and *B* sites at the room temperature, which results in the increase of μ_{ferri} with *Mn* content(x) and therefore may leading to increase M_s and associated H_c. The increasing trend in μ_{ferri} is the signature of ferri-to-ferro and decreasing trend of ferri-to-para magnetic phase transitions for *Co* substituted and *Fe* substituted compositions respectively. But $\mu_{ferri}$is found to increase for $Co_{1+x}Mn_xFe_{2-x}O_4$as shown in Figure 6 because of concurrent addition of *Co* along with *Mn* substitution for *Fe,* which may lead to supersede the effect of longer hopping lengths through the formation of new probable phases due to more influence of inherent ferromagnetic ordering of *Co* in this system. This is found in agreement with the recently published experimental result [10, 14]. Thus this eventual variation ofμ_{ferri} leads to predict that thermally fluctuated magnetic ions require more thermal energy (κT) in$Co_{1-x}Mn_xFe_2O_4$ (where *Mn* substituted for *Co*) than in$CoMn_xFe_{2-x}O_4$ (where *Mn* substituted for *Fe*) to decrease spontaneous magnetization, which is indicative to make T_C tunable by adjusting *Mn* content and almost in agreement with published experimental result[13]. As the particle size reduces to the nanoscale (typically <20nm) range, '*a*' increases with the Laplace pressure difference [11] and eventually may decrease μ_{ferri} due to increase of hopping length. Hence, counterbalance of μ_{ferri} may be possible in$Co_{1-x}Mn_xFe_2O_4$ by adjusting *Mn* content, which may lead to tune T_C or T_N at an optimum point for making superparamagnetism (*SPM*)tunable closer to the room temperature.

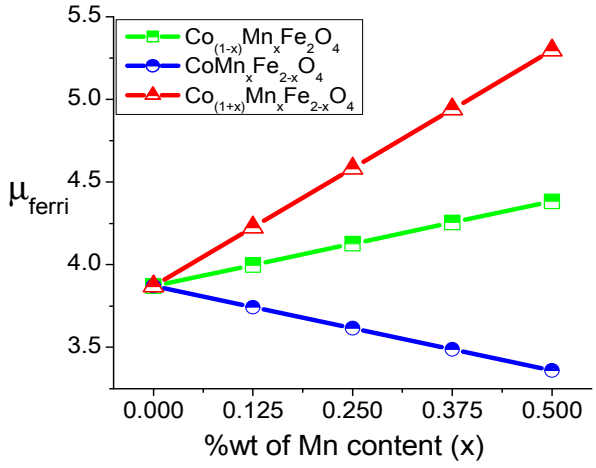

Figure 6. *Effective magnetic moment, μ_{ferri} as a function of Mn content.*

3.3. Magneto-Mechanical Properties

The magneto-mechanical property includes the magnetoelastic and magnetostriction properties of magnetic materials. Magnetoelastic property is also known as inverse magnetostriction, which refers to the change of magnetization with mechanical stress. The stress may develop from strain during synthesizing the material. This strain is closely related to the bond length in ferromagnetic materials. As such the increase of bond lengths both in *A* and *B* sites may decrease *A-A* and *B-B* interactions in $CoMn_xFe_{2-x}O_4$ but increase *A-A* and *B-B* interactions with the decrease of bond lengths in$Co_{1-x}Mn_xFe_2O_4$ and resulting increase in the magnetization of the later. The shape or dimension of the material may have a phenomenological relationship with the bulk density, which in turn a measure of porosity of the ferromagnetic material. The longer is the bond length, the higher is the porosity and vice versa. Accordingly, the lower is the magnetization, the higher is the porosity and vice versa. As such, $CoMn_xFe_{2-x}O_4$ may exhibit higher porosity compared to $Co_{1-x}Mn_xFe_2O_4$as reported [15]. But in $Co_{1+x}Mn_xFe_{2-x}O_4$, higher porosity might be observed due to the probable formation of new phases during synthesizing and therefore more suitable for magneto-mechanical sensor applications, which is also a subject to further experimental investigation. The imaginary part of magnetic susceptibility is responsible for converting

magnetic energy into heat in a fluid when exposed to an alternating field, which is governed by the relaxation process. The relaxation time, τ determines the maximum achievable loss power as reported [16]. Apart from the field parameter, the power loss is related to the susceptibility of the materials of nanoparticles, which again depends on saturation magnetization, particle volume, and field amplitude. With required particle size, this saturation magnetization might be controlled to an optimum value of temperature by adjusting *Mn* doping in $Co_{1-x}Mn_xFe_2O_4$, which may be suitable for use in magnetic hyperthermia to destroy the cancer cells without much damaging of neighbor cells. Thus, mostly impact of *Mn* content on lattice constant, hopping and bond lengths, magnetic moment, Curie temperature and porosity has been discussed in this analytical study to predict the controlling of magnetization, magneto-mechanical property and SPM by an external agent like ambient or operating temperature, applied magnetic field adjusting dopant (*Mn*) content. Besides, the materials require high resistivity, high permeability, and low dielectric loss over a wide range of frequencies for high frequency applications. *Mn* doped cobalt ferrite may meet such requirement of high resistivity with $CoMn_xFe_{2-x}O_4$ and $Co_{1-x}Mn_xFe_2O_4$ because *Mn* has less electrical conductivity compared to both *Co* and *Fe,* used to substitute them. However, the analysis and findings are completely based on the theoretical aspect of this paper and need experimental verification to confirm and supplement the prediction.

4. Conclusion

Three systems of *Mn* doped cobalt ferrite with composition formula $Co_{1-x}Mn_xFe_2O_4$, $CoMn_xFe_{2-x}O_4$, and $Co_{1+x}Mn_xFe_{2-x}O_4$ have been undertaken for analytical study in a theoretical approach. In that$Co_{1-x}Mn_xFe_2O_4$ exhibits the decrease of lattice constant with *Mn* content substitute for *Co* whereas $CoMn_xFe_{2-x}O_4$ and $Co_{1+x}Mn_xFe_{2-x}O_4$ exhibit to increase the lattice constant, substituted for *Fe*. The estimated bond and hopping lengths demonstrate the variation similar to the lattice constant with *Mn* content. The magnetic moment increases in $Co_{1-x}Mn_xFe_2O_4$ with *Mn* content due to shortening of hopping lengths but in $CoMn_xFe_{2-x}O_4$, the magnetic moment decreases due to the increase of hopping lengths with *Mn* content. The increasing trend of μ_{ferri} may be indicative for ferri- to-ferro magnetic phase transition in $Co_{1-x}Mn_xFe_2O_4$ and $Co_{1+x}Mn_xFe_{2-x}O_4$ whereas the decreasing trend for ferri-to-para magnetic phase transition in $CoMn_xFe_{2-x}O_4$. The increase in lattice constant according to Laplace pressure difference is also expected in all three systems undertaken for analytical study when the size of the particle reduces to the nanoscale. For $Co_{1-x}Mn_xFe_2O_4$, it might be possible to control and tune M_s and T_C by adjusting *Mn* content and the particle size depending on the synthesizing method. This is a unique and significant property for $Co_{1-x}Mn_xFe_2O_4$, which may make it suitable for advanced applications like magnetic hyperthermia etc. whereas in the other two compositions, reducing of particle size to nanoscale may increase the porosity due to lengthening of *A-O* and *B-O* bond lengths by affecting on bulk density and may make them suitable for environmental sensors. However, since the analysis is completely based on theoretical aspects, so further investigations with synthesized samples of these compositions are required to supplement and confirm the findings and results to assess suitability for advanced applications in the days to come.

Acknowledgements

The authors are thankful to the ISP (International Science Programs), Uppsala University, Sweden for financial and technical support, and also to the department of physics, Bangladesh University of Engineering and Technology for experimental support.

References

[1] S. Bawawaje, M. Hashi, I. Ismail, J. Magn. Magn. Mater, 323 1433 (2011).

[2] R. Ahmad, I. H. Gul, M. Zarrar, H. Anwar, M. B. Khan Niazi, A Khan, J. Magn. Magn. Mater, 405 (2016), pp. 28-35.

[3] Y. D. Kolekar, L. Sanchez, E. J. Rubio, C. V. Ramana, Solid State Communications, 184 (2014), pp. 34-39.

[4] N. Sivakumar, ANarayanasamy, C. N. Chinnasamy, B. Jeyadevan, J. Phys. Cond. Mat., 19 (38), (2007), pp. 386201-386211.

[5] N. Ponpandian, P. Balaya, A. Narayanasami, Journal of Physics: Condensed Matter 14 (2002), 3221.

[6] H. Kumar, R. C. Srivastava, J. P. Singh, P. Negi, H. M. Agrawal, D. Das, K. HwaChae, J. Magn. Magn. Mater, 401 (2016), pp. 16-21.

[7] S. Exvier, S. T. Binu. P. Jacob, E. M Mohammed, journal of Nanoscience, 1, (2013).

[8] M. Z. Ahsan, F. A. Khan, Journal of Physical Science and Application (2017), doi: 10.17265/2159-5348/2017.06.005.

[9] D. S. Mathew, R. S. Juang, Chemical Engineering Journal, 129, 51, (2007).

[10] J. P. Singh, H. Kumar, A. Singhal, N. Sarin, R. C. Srivastava, K. H. Chae, Appl. Sci. Lett. (2016) DOI: 10.17571/appslett.2016.02001.

[11] L. Blaney, Magnetite (Fe_2O_4): Properties, synthesize and applications, Lehigh University, volume-15, (2007).

[12] S. Singhal, T. Namgya, S. Bansall, K. Chandra, J. Electromagnetic Analysis & Applications, 2, 376, (2010).

[13] O. Caltan, L. Dumitru, M. Feder, N. Nupu, H. Chiriac, J. Magn. Magn. Mater, 320, 869, (2008).

[14] M. Z Ahsan, F. A Khan, Mater Sci. Nanotechnol., 2 (2), 1 (2018).

[15] A. Khan, M. A. Bhuiyan, G. Dastagir, A. Quaderi, K. H. Maria, S. C. Choudhury, K. M. A. Hossain, S. Akhtariand D. K. Sahai, Journal of Bangladesh Academy of Sciences, 37 (1), 73, (2013).

[16] A. H. Habib, C. L Ondeck, P. Chudhary, B. R Bockstaller, and M. E McHency, J. Appl. Phys., 103, 07, (2008).